

Outdoor Millimeter-Wave Channel Modeling for Uniform Coverage Without Beam Steering

M. Sheeba Kumari¹(✉), Sudarshan A. Rao², and Navin Kumar³

¹ New Horizon College of Engineering, Bangalore, India
sheeba.bnm@gmail.com

² BigSolv Labs Pvt Ltd., Bangalore, India
dr.sudarshan.rao@ieee.org

³ Department of ECE, Amrita School of Engineering, Amrita Vishwa Vidyapeetham University,
Bangalore, India
navinkumar@ieee.org

Abstract. Diverse performance requirements of the emerging 5G cellular systems and their deployment challenges motivate researchers to explore high frequency millimetre wave (mmWave) spectrum as a potential solution. The allocation and utilization of mmWave spectrum in cellular communication is a new frontier. In this paper, we investigate a directional mmWave small cell outdoor propagation channel by exploiting its deterministic nature; using ray tracing method. Estimates on specific attenuation measurements and free space propagation parameters reveal that directional transmission is inevitable and would result in a channel model divergent from that of an omnidirectional propagation model. In addition, we examine the effect of antenna tilting in the access links to establish highly directional adaptive link. Capacity of the sparsely faded channel is also analyzed. Results exemplify that, beyond 50 m propagation range, the received signal strength in mmWave small cells employing base stations of height 5 m as opposed to macro cells with base station height of 20 m is independent of beam steering. A simplified geometry devoid of the complexity of adaptive beam steering is hence proposed to provide uniform signal strength in an outdoor small cell channel to affirm low latency.

Keywords: 5G · mmWave · Ray tracing · Channel model · Beam steering

1 Introduction

Upcoming 5G cellular communication system with its claim for higher data rate as well as lower latency motivates the use of mmWave frequency spectrum to meet the desired performance specifications [1, 2]. The wide bandwidth available at these high frequencies eliminates spectrum shortage, a major concern in currently deployed cellular systems. Contrary to the fragmented spectrum available in long term evolution (LTE) standards, large contiguous spectrum of approximately 200 GHz enhances the acceptance of mmWave spectrum in cellular communication. The short wavelength of mmWaves (1 to 10 mm) grants integration of many antennas into the same physical dimension, enabling massive multiple input multiple output (MIMO) technique.

However, mmWave signals even with the promised high data rate are confined to short communication range due to high free space path loss [3]. The transmission is additionally affected by atmospheric variations such as rain, fog and other moisture content present in the atmosphere. Unlike the traditionally evolved pre-5G technology, mmWave based 5G introduce significant engineering challenges; starting with an accurate analysis of mmWave propagation channel. The channel characteristics vary for diverse propagation scenarios leading to varying system performance. Hence, massive research is driven to assess this technology in 5G context essentially with directional antennas to offer significant extension of link distance than would omnidirectional antennas [4–9]. Initial estimates revealed that signal outages become prominent beyond 200 m. This serves to realize small cell structures with ease contributing to the network densification paradigm.

Ongoing investigations explore diverse methods to model mmWave channel [5–9], improve coverage and capacity [7], exploit beam forming techniques [3] and design network architecture [10]. Path loss data for distinct mmWave frequencies of 28 GHz and 73 GHz are presented in [4] for the perusal of researchers to analyse mmWaves. However, a major work is based on modelling the channel statistically or empirically which lacks accuracy or generality respectively. Computationally complex deterministic modelling can be simplified for the mmWave case due to relatively low dense multipath components [7–9]. Additionally, they assist beam forming techniques through real time estimation of link's directional parameters eliminating the need for extensive beam switching search techniques. Though beamforming technique enhances system gain, its practical implementation involves acquiring comprehensive channel state information. Also, 5G networks due to their smaller cell size have increased handoff probability. The observation, that implementing complex adaptive beam steering technique frequently would affect the latency of the network, is the motivation for this paper. Ray tracing for an mmWave indoor model is demonstrated in [8] and outdoor channel modelling with six ray model is presented in [7, 9]. Yet the models were not fitted in with beam steering technique. Channel characteristics at 60 GHz were examined in [7] whereas [9] explored the entire mmWave spectrum. However, the model geometry in either case was limited to the backhaul transmission.

In this paper, a ray tracing channel model is used to analyse mmWave propagation characteristics for two different use cases namely, wireless backhaul and cellular access. The outdoor base stations implemented with backhaul provisioning, have predictable point to point channel geometry. This, as well as a sparsely populated access channel scenario is modelled using simple deterministic radio channel model. We assumed highly directional horn antenna at both transmitting and receiving sides to assess the received signal strength. The increased outage probability in access channel for regions close to the transmitting antenna is further corrected using beam steering. Beam tilt angle synthesized from the cell geometry is successively updated in the model. Though the probability of deep fade reduces with beam steering, the mmWave link quality excepting beamsteering was observed to be significant at receiver locations beyond 50 m. Hence, we propose a simple layout of 2×2 MIMO for a low latency moderate data rate mmWave system, with one pair of antenna, aligned along the boresight and another pair oriented at an angle. Hence a minimal of two orientations in the elevation plane and the beam

swept over the entire azimuth plane suffices to provide uniform coverage in the cell area. This is possible under the assumption of a small cell network with non-blockage, employing base stations/access points at a nominal height of 5 m–8 m. The suggestion is analytically validated by evaluating antenna tilt at all locations within the cell range in distinct steps. Furthermore, the channel capacity of the fading channel is analysed and compared for spatial diversity.

Rest of this paper is organized as follows. Section 2 discusses the propagation characteristics of mmWave channel. mmWave outdoor propagation model is elucidated in Sect. 3 highlighting the antenna design and beam steering strategy. All the results together with significant discussions are provided in Sect. 4. The conclusive statements are included in Sect. 5.

2 Propagation Characteristics of mmWave Channel

2.1 Propagation Characteristics

The propagation characteristics of mmWaves vary from that of existing microwaves and may appear adverse for cellular communication; given the increased propagation loss affiliated with such high frequencies. However, the increase in path loss is supportive for small cell design which increases cellular capacity. Also, the increased pathloss can be compensated by increasing the directivity of antenna, if desired; leading to high effective isotropic radiated power for the same transmitted power levels. To have realistic estimation of channel propagation, it is essential to consider atmospheric absorption loss of mmWaves while evaluating the received signal strength. The empirical model developed by Liebe [11] and the approximate model proposed by ITU-R [12] are two popular techniques. The complex Liebe's model calls for empirical parameters obtained from laboratory measurements to estimate the absorption coefficient whereas the approximate model is based on a rather straight forward approach and is used where accuracy is compromised for simplicity. The modified received power is given by [15]:

$$P_{r,dBm}(min) = P_{t,dBm} + G_{t,dBi} + G_{r,dBi} - L_{dB} \quad (1)$$

where, P_t and P_r represent the transmit and receive power, G_t and G_r the transmitter and receiver gain factor respectively in dBi and L represents the path loss in dB. The total path loss is given as:

$$L_{dB} = L_{FSL,dB} + L_{abs,dB} + L_{Margin,dB} \quad (2)$$

where, L_{FSL} is free space path loss, L_{abs} is the absorption loss and L_{Margin} is the link margin.

2.2 mmWave Link Budget

The simulation is conducted for a 2 Gbps QPSK link, maximum 200 m link range, having a minimum Eb/N0 of 12 dB and a channel bandwidth of 1.5 GHz. The choice of link distance is made to budget for a distance which, even in worst case would result in a

tolerable path loss. Using the above parameters, to obtain an un-coded bit error rate (BER) of less than 10^{-7} , the required signal-to-noise ratio (SNR) is 14 dB. For a nominal receiver noise figure of 3 dB, the receiver sensitivity is -65.5 dBm. This value is used as the free space benchmark in our simulations and is the threshold for examining outage probability. The directional antenna is designed for 21.6 dBi directivity. Applying oxygen absorption loss of 16 dB/km, the loss for 200 m link is 3.2 dB. For an additional link margin of 5 dB, we establish that the transmit power is 13.5 dBm for 60 GHz transmission. The maximum allowable path loss is thus budgeted as 114.3 dB using the equation [13]:

where, $EIRP$ represents the effective isotropic radiated power obtained as 35.14 dBm,

$$PL_{dB}(max) = EIRP_{dBm} - P_{r,dBm}(min) - L_{dB} + G_{dBi} \quad (3)$$

$P_{r,dBm}(min)$ represents the receiver sensitivity, L_{dB} represents the absorption loss together with the link margin in dB and G represents the receiver gain factor in dBi.

3 Proposed Channel Model

mmWave system performance is well analyzed with a suitable propagation model that captures major propagation challenges including higher carrier frequency, wider bandwidth, larger antenna array elements and directional transmission. In this work, we used a deterministic ray tracing model employing highly directional horn antenna to generate narrow beam signals resulting in sparser multipath components (MPCs).

3.1 Antenna Design

This work assumes a highly directional horn antenna with side lobe level 14 dB lower than the main lobe peak and having a beam width of 13° and 15° at half power in the elevation and azimuth planes, respectively.

$$G(\phi, \theta) = G_0 [\text{sinc}^2(a \cdot \sin(\phi)) \cos^2(\phi)] \cdot [\text{sinc}^2(b \cdot \sin(\theta)) \cos^2(\theta)] \quad (4)$$

Equation (4) avoids analytical solving of complex double integration [14] wherein $G(\phi, \theta)$ is the antenna gain at azimuth and elevation angles respectively, G_0 represents the peak gain at antenna boresight which occurs for a value of $\phi = \theta = 0$. The constants a and b were estimated using azimuth and elevation HPBW's for normalized half power values.

3.2 Six Ray mmWave Channel Model

The directional mmWave outdoor channel with reduced MPCs has been modeled as a six ray street canyon (SC) model. The direct ray (LOS), ground reflection, first order reflections from either side of the walls and additional second order reflections from both the walls forms the six multipath components. The specific backhaul geometry chosen is an outdoor link with transmitting and receiving nodes deployed on lamp-posts

separated by 200 m as in Fig. 1. (Ground reflection is analyzed, but not shown in the illustration due to limitation on dimensionality.) The assumption of closely placed multi-storey buildings [7] helps to treat the buildings on either side of the street as a single reflecting wall resulting in worst case reflection scenario leading to maximum signal attenuation. The effect of diffraction from building edges, due to its insignificance in mmWave links, is excluded in the analysis. The model parameters assumed in channel simulation are listed in Table 1.

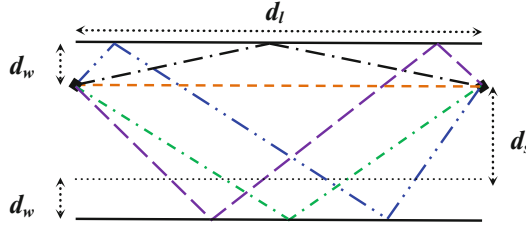


Fig. 1. Top-down view of street canyon six ray propagation geometry.

Table 1. Model parameters for ray tracing channel simulation.

Simulation parameter	Unit	Value
Link range (d_l)	m	200
Transmitting frequency	GHz	60
Width of the street (d_s)	m	12
Transmitter to wall distance (d_w)	m	4
Receiver to wall distance (d_w)	m	4
Antenna gain	dBi	21.6

For six ray channel model, the MPCs contributing to the total response are:

$$h = h_{Los} + h_g + \sum_{i=1}^M h_i \quad (5)$$

where h_{Los} , h_g and h_i are the contributions of the LOS, ground reflected and first/second order wall reflected paths respectively. M represents the total number of wall reflections, having a value of 4 in the six ray model accounting for 2 single and double reflections each. The directional mmWave channel impulse response is hence expressed as:

$$h(f, \theta, \varphi) = G_{Los}(\theta, \varphi)H_{Los} + G_g(\theta, \varphi)H_g + \sum_{i=1}^M G_i(\theta, \varphi)H_i \quad (6)$$

where $G_{Los}(\theta, \varphi)$, $G_g(\theta, \varphi)$ and $G_i(\theta, \varphi)$ are the products of transmit and receive antenna power patterns for LOS, ground reflected and i^{th} wall reflected rays at appropriate elevation and azimuth angles evaluated from (4) and H_{Los} , H_g and H_i are their channel impulse response components,

$$\begin{aligned} H_{Los} &= \left[\frac{\lambda}{4\pi p_{Los}} e^{(-K_p p_{Los}/2)} \right] e^{\left(-j \frac{2\pi}{\lambda} p_{Los} \right)} \\ H_g &= \left[\Gamma_g \frac{\lambda}{4\pi p_g} e^{(-K_p p_g/2)} \right] e^{\left(-j \frac{2\pi}{\lambda} p_g \right)} \\ H_i &= \left[\Gamma_i \frac{\lambda}{4\pi p_i} e^{(-K_p p_i/2)} \right] e^{\left(-j \frac{2\pi}{\lambda} p_i \right)} \end{aligned} \quad (7)$$

where λ is the wavelength, p_{Los} , p_g and p_i are the path lengths of LOS, ground reflected and first/second order wall reflected paths respectively, Γ_g and Γ_i are the reflection coefficient for ground and wall reflections, K_p is the coefficient for exponential absorption and $2\pi/\lambda$ is the wave number.

The mmWave sparsely faded channel characterization can be obtained as follows:

- (1) Generate mmWave SISO channel model from Eq. (8) for the given outdoor street canyon geometry using the path lengths of MPCs and their related AoAs and AoDs taking antenna directionality into account. Analyze the received power for wireless backhaul with antenna height fixed at 5 m.
- (2) Adapt the model to accommodate receiver antenna height of 1.5 m to explore access link. To perform antenna beam steering, change the orientation of antenna radiation pattern through ongoing tilt angle calculation, using Eq. (9).
- (3) Compute the CIR contributions $h_{m,n}$ from the n th transmit antenna to the m th receive antenna to determine the MIMO channel matrix H . The multipaths with AoAs and AoDs within the antenna beam solid angle are used in evaluating the response.
- (4) Obtain the MIMO channel capacity relative to the free space signal to noise ratio (SNR_{LOS}):

$$C = \log_2 \left| I_{N_r} + \frac{SNR_{LOS}}{N_t} HH^H \right| b/s/Hz \quad (8)$$

where N_r and N_t are the number of receive and transmit antennas, I_{N_r} refers to $N_r \times N_r$ identity matrix, SNR_{LOS} refers to signal-to-noise ratio relative to LOS and HH^H refers to the matrix product of MIMO channel matrix and its Hermitian.

3.3 Beamsteering vs Non-beamsteering

In backhaul analysis, the antenna placed on either lamp post at a height of 5 m is oriented along the boresight. However, for wireless access channel characterization, the receiver is assumed at a height of 1–2 m which for optimal performance suggests the transmitter

(AP) antenna radiation pattern to be tilted down by an angle $\Delta\theta$ with respect to horizontal axis. The channel model performance with beamsteering is hence investigated by tilting the main beam of BS and user equipment (UE), leading to main lobes aligned for maximum received signal strength. Thus, by varying the antenna tilt angle for Tx-Rx pair in the model, a direct link with maximum antenna gain is created from the transmitter to the receiver for every receiver locations. The tilt angle is obtained from the vertical angle between BS antenna and UE antenna given by:

$$\Delta\theta = \arctan(h_t - h_r/d) \quad (9)$$

where h_t and h_r are the heights of transmitting and receiving antenna respectively and d is the distance of separation between them. The concept of SISO hitherto explained can be extended to simulate transmit/receive diversity or MIMO to enhance performance.

Though beamforming in MIMO enhances channel performance in terms of extended coverage as well as reduced deep fades, it requires smart signal processing algorithms to estimate spatial signature like direction of arrival (DoA) of the signal increasing the system's complexity. For small cells, with cell radius typically below 200 m and access points/BS mounted at relatively low heights as in the modeled channel geometry the tilt angle variation is trivial. Alternately, we propose a simplified geometry, in Fig. 2, wherein the antenna array with two elements at the lampposts is oriented differently leading to uniform coverage with interference mitigation traded off. A pair of array elements on either lamppost is oriented horizontally to serve the small cell backhaul link as well as the UE far from the transmitter say, at the cell edge. The UE position in the proximity of lamp post, outside the antenna beam width, receives signal from the second antenna element oriented at an angle of 15° relative to boresight.



Fig. 2. Proposed small cell layout geometry devoid of beamsteering for uniform coverage.

4 Results and Discussion

First, we compare the absorption loss simulated for mmWave E-band frequencies using two standard modeling methodologies listed in Sect. 2 [11, 12]. As illustrated in Fig. 3, we observe that variations in attenuation due to oxygen absorption for the models are less than 0.3 dB/km for frequencies in the upper E-band. Even at the frequency of interest, 60 GHz, the observed variation is not more than 0.62 dB/km leading to our choice of approximate model. The high attenuation value of 16 dB/km obtained justifies

the suitability of 60 GHz mmWave band in limited communication range small cell network design. The normalized antenna radiation pattern for a horn antenna used in the channel model simulation is shown in Fig. 4. This reference antenna model forms the basis for evaluating the MPCs’ strength at each pointing angle (AoAs and AoDs) which in turn is obtained through ray optic analysis of street canyon geometry. The antenna being vertically polarized, E-plane and H-plane determine the antenna gain factor for ground and wall reflections respectively. Note that 0° implies horizontal orientation of beam along the reference. The constants a and b are evaluated as 3.35 and 3.88 by equating Eq. (4) to $1/2$, solving for ϕ and θ respectively. The narrow beam width of receiving antenna guarantees that a reflected path greater than second order is either received outside the beam area or attenuated significantly relative to LOS ray. The simulated results demonstrate that six ray channel modeling suffices directional mmWave channel characterization for the chosen geometrical layout (refer Fig. 8).

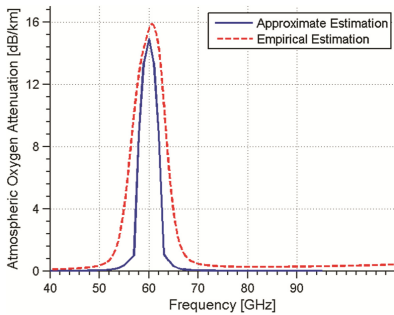


Fig. 3. Specific attenuation simulated using Leibe’s model and approximation model.

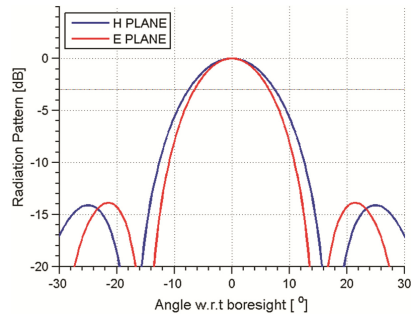


Fig. 4. Normalized power pattern for a horn antenna, $HPBW\phi = 15^\circ$ and $HPBW\theta = 13^\circ$.

The backhaul channel is analyzed by placing in the frequency dependent absorption loss and angle dependent antenna gain factor. Figure 5 depicts received signal variations observed in backhaul ecosystem wherein transmitting and receiving antennas are mounted on lampposts at 5 m from the ground and 200 m apart. As illustrated, the variation in faded signal strength with respect to free space benchmark is more for link distances exceeding 100 m with the deepest fade of -99.09 dBm occurring at 123 m. This is due to the existence of all the higher order reflections. The mmWave link up to a range of 30 m is predominantly LOS with zero contribution from reflected rays as their AoAs fall outside the beamwidth leading to a non-faded channel. The significant variation of received power owes to the small wavelength of mmWave carrier signal. Another relevant aspect is the reduced deviation of the statistical distribution from its free space value below 100 m.

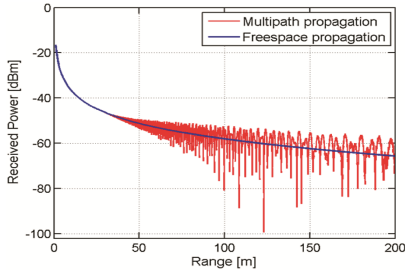


Fig. 5. With antenna aligned at the boresight for backhaul ecosystem.

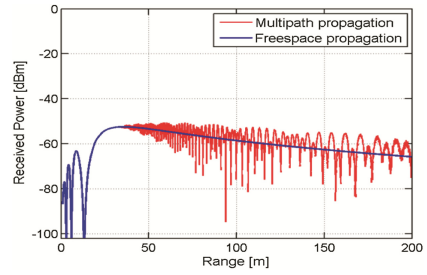


Fig. 6. Antenna aligned at the boresight for cellular access.

The signal strength in access network analysed for a receiving antenna height of 1.5 m with antenna radiation pattern aligned horizontally is shown in Fig. 6. It is analogous to the backhaul case for Tx-Rx separation distance greater than 36 m. For the chosen antenna beamwidth and the small cell geometry, the pattern spans such that even a horizontally aligned beam ensures signal reception. It is also observed that at distance closer to the lamp post signal outage occurs suggesting the need for beam steering. The beam is hence adaptively tilted by an angle generated by Eq. (6) to correct the probability of signal outage. The resulting received signal strength variations can be easily compared from Figs. 6 and 7. Hence, we observe that the probability of fade at the close-in distance of transmitting antenna is corrected with beam steering. The comparison between simulated six and eight ray models, in terms of relative received power level in dB, for varying cases of backhaul and access transmissions is presented in Fig. 8. When transmitting and receiving antennas were assumed to be of same height, introducing two additional reflections at the receiver had negligible impact. This illustrates the triviality of the number of reflecting bodies in a directional transmission scenario. The statistical distribution of received power in six ray model for the chosen geometry is observed to be identical to eight ray model with 89% of the mmWave links. For the access case, variation between two models is more apparent indicative of choosing higher order ray tracing model. However, as the difference is less than 10 dB for 90% of the links, we reckon six ray models as a fair approximation for mmWave channel propagation characterization.

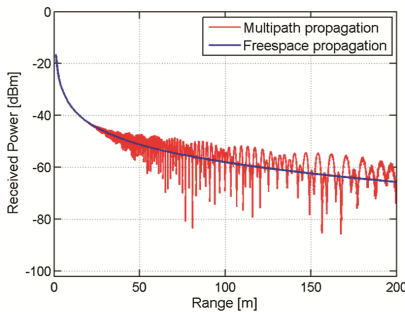


Fig. 7. Rx signal strength with appropriate antenna alignment using beam steering.

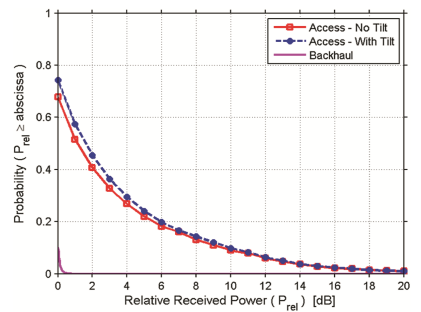


Fig. 8. Adequacy of six ray model to characterize mmWave link is depicted.

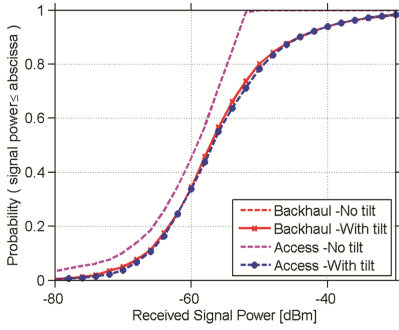


Fig. 9. Probability of signal strength required analyzed for diverse cases.

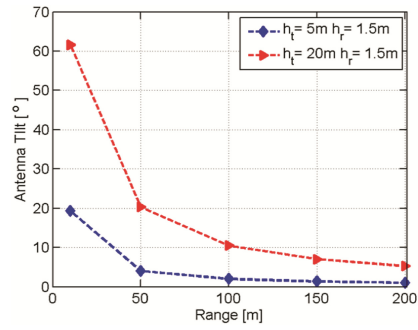


Fig. 10. Antenna tilt angle to maintain the beam orientation.

The cumulative distribution function (cdf) plot (Fig. 9) shows that the probability of received signal fitting in a precise range, for backhaul and access case, is approximately same even with adequate inclination of antenna beam to route energy in the desired direction. It is depicted that without antenna tilt, signal strength for a given transmission link within the cell coverage area is always less than -52 dBm. Yet, this value is higher than the free space signal benchmarked at -65.5 dBm. The antenna tilt technique adapted offers a direct LOS link aligned with the strongest signal. It may be noted that the model, for convenience, in analysis assumes an un-obstructed LOS link. The tilt angle evaluated for two different cases, first being with the proposed height of 5 m and second with the traditional BS height of 20 m, is provided in Fig. 10. For a small cell of size 200 m, employing base station on lamp posts or like structures, a tilt is required primarily in the serving area close to the base station. The results show that in addition to the antenna beam oriented along the horizontal direction, it may be sufficient to have a single additional beam tilted by an angle in the range $[5^{\circ}-15^{\circ}]$ with respect to horizontal to provide uniform signal strength at any UE location within the cell area of radius 200 m.

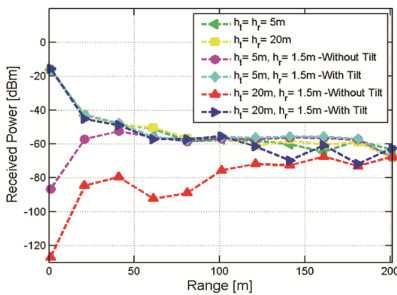


Fig. 11. SISO received power compared to emphasize proposed antenna tilt strategy.

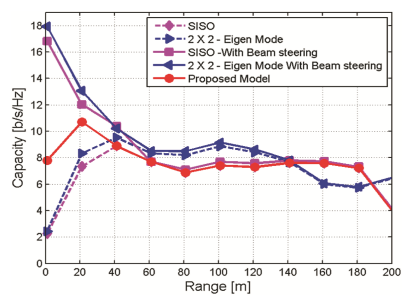


Fig. 12. Capacity analysis of access channel.

The received signal power at distinct receiver locations within the selected link range are presented in Fig. 11. We learn that significant reduction in received power is observed

only when the access points are placed high above ground level, say 20 m, for receiver located anywhere in the cell range. Else, except for the deep fades at certain receiver locations, the statistical distribution of received signal strength is approximately uniform even in the absence of beam steering. The proposed method hence demonstrates a simple and viable solution for effective transmission in a cell layout where LOS condition prevails. The capacity of access channel is analysed in the presence and absence of beam steering and compared with the proposed model in which beam is oriented in two fixed directions. The analysis is conducted with a static beam oriented at a tilt angle of 15° with respect to horizontal. It is observed that though the model architecture yields a uniform capacity over the entire range even though it fails to acquire the peak rates offered by steerable antenna at low link ranges (Fig. 12).

5 Conclusion and Future Work

mmwave exhibits the prospective for use as small cell backhaul and access in upcoming 5G cellular networks. Antenna patterns and specific attenuation due to atmospheric absorption are to be considered to derive an accurate directional mmWave channel model. Steering the beams toward major paths and/or the nulls toward interfering paths will minimize interference to an extent where even the MPC that contributes destructively can be phased out. We examine a six ray model with directional transmission incorporating antenna steering to evaluate the received signal strength for cellular backhaul and access networks. The probability of fading for backhaul channels, irrespective of antenna steering is observed to be approximately 9%. An equivalent fading probability is realized for access channels incorporating antenna steering. However, an increased outage probability of 17% is obtained for access channel without antenna tilting. Our mmWave signal strength study indicates that incorporating beamsteering in an outdoor small cell street canyon channel hence offers an 8% enhancement in the channel performance.

This study on antenna angle-dependent mmWave channel model assimilates the directionality and steerability of mmWaves. Hence, for the chosen channel specification, significant performance is assured in a small cell network with simple antenna geometry of two guided beams at the transmitting base station trading off the aforementioned 8% performance enhancement. Yet, in a deployment scenario of highly populated urban area with large number of buildings and moving vehicles, such an approximation may not work and have to be analyzed using a site generic probabilistic model to capture the channel characteristics effectively. Hence, with small cell size and reduced Tx antenna height, we demonstrate that adequate performance is guaranteed with two different vertical orientations of the transmitting antenna. The model can be extended to analyze higher order multipath components.

References

1. Sadri, A.: mmWave technology evolution: from WiGig to backhaul and access for 5G. In: Proceedings of International Workshop on Cloud Cooperated Heterogeneous Networks, Osaka (2013)
2. Warren, D., Dewar, C.: Understanding 5G: perspectives on future technological advancements in mobile. White paper, GSMA Intelligence (2014)
3. Rappaport, T.S., et al.: Millimeter wave mobile communications for 5G cellular: it will work! *IEEE Access* **1**, 335–349 (2013)
4. Maccartney, G.R., Rappaport, T.S., Samimi, M.K., Sun, S.: Millimeter-wave omnidirectional path loss data for small cell 5G channel modeling. *IEEE Access* **3**, 1573–1580 (2015). ISSN 2169-3536
5. Sun, S., et al.: Synthesizing omnidirectional antenna patterns, received power and path loss from directional antennas for 5G millimeter-wave communications. In: Proceedings of IEEE Global Communications Conference, GlobeCom 2015, pp. 1–7. IEEE Press (2015)
6. Rappaport, T.S., MacCartney Jr., G.R., Samimi, M.K., Sun, S.: Wideband millimeter wave propagation measurements and channel models for future wireless communication system design. *IEEE Trans. Commun.* **63**(9), 3029–3056 (2015)
7. Zhang H., Venkateswaran, S., Madhow, U.: Channel modeling and MIMO capacity for outdoor millimeter wave links. In: Proceedings of IEEE Wireless Communications and Networking Conference, WCNC, pp. 1–6. IEEE Press (2010)
8. Steinmetzer, D., Classen, J., Hollick, M.: mmTrace: modeling millimeter-wave indoor propagation with image-based ray-tracing. In: Proceedings of Millimeter wave Networking Workshop, mmNet 2016 (2016)
9. Kumari, M.S., Rao, S.A., Kumar, N.: Characterization of mmWave link for outdoor communications in 5G networks. In: Proceedings of IEEE International Conference on Advances in Computing, Communications and Informatics, ICACCI, pp. 44–49. IEEE Press (2015)
10. Gotsis, A., Stefanatos, S., Alexiou, A.: UltraDense networks: the new wireless frontier for enabling 5G access. *IEEE Veh. Technol. Mag.* **11**(2), 71–78 (2016)
11. Liebe, H.J.: MPM-An atmospheric millimeter-wave propagation model. *Int. J. Infrared Millim. Waves* **10**, 631–650 (1989)
12. ITU-R Recommendation: Attenuation by atmospheric gases. ITU-R P.676-11 (2016)
13. Madhow, U.: Introduction to Communication Systems. Cambridge University Press, Cambridge (2014)
14. Far field radiation from electric current. <http://www.thefouriertransform.com/applications/radiation.php>
15. Goldsmith, A.: Wireless Communications. Cambridge University Press, Cambridge (2005)